

Sizing Criteria for Traction Drives

Douglas A. Rohn,* Stuart H. Loewenthal,* and John J. Coy†

The development of reliable, lightweight, high-power traction drives for aerospace and terrestrial applications is rapidly expanding. Adjustable-speed drives have been used in a variety of commercial applications for over 50 years. Recent improvements, in terms of fluids with higher traction, materials with greater fatigue resistance, and design techniques with greater accuracy, have helped to increase their performance and reliability.

When designing or selecting a traction drive, one must be concerned with the service life of the unit. Presently, very little fatigue life data are available from well-controlled traction contact fatigue tests. However, many investigations have been conducted on rolling-element fatigue for rolling-element bearings (ref. 1). Because of the similarity in the expected failure mode, namely, rolling-element fatigue, the life analysis methods used to establish rolling-element bearing capacity ratings should be applicable to determining the service life and capacity of traction drive contacts (ref. 2).

The purpose of this paper is to present a simplified traction drive fatigue analysis (ref. 3), which was derived from the Lundberg-Palmgren theory (ref. 4). A second objective is to use this analysis to investigate the effects of rotational speed, multiplicity of contacts, and variation in the available traction coefficient on traction-drive system life, size, and power capacity. Some of these effects were studied in reference 3. Simplified equations are provided for determining the 90 percent survival life rating of steel traction-drive contacts of arbitrary geometry. References to life-modifying factors for material, lubrication, and traction will be made.

Symbols

a	contact ellipse semimajor axis, m (in.)
a^*	dimensionless contact ellipse semimajor axis
b	contact ellipse semiminor axis, m (in.)
b^*	dimensionless contact ellipse semiminor axis
c	orthogonal shear stress exponent
E	modulus of elasticity parameter, Pa (psi)
E'	material elasticity parameter, Pa (psi)
e	Weibull exponent
F	relative curvature difference
g	auxiliary elliptical contact size parameter, m (in.)
H	drive system life, hr
h	depth to critical stress exponent
K_1	material constant
K_2	geometric life variable
L	life, millions of stress cycles
N	number of planet rollers
n	speed of rotation, rpm
Q	rolling body normal load, N (lbf)
R	rolling radius, m (in.)
r	radius, m (in.)
u	number of stress cycles per revolution

*NASA Lewis Research Center.

†Propulsion Laboratory, U.S. Army Research and Technology Laboratories (AVRADCOM), NASA Lewis Research Center.

- V stress volume, m³ (in.³)
 W roller width, m (in.)
 z_0 depth to critical stress, m (in.)
 μ traction coefficient
 μ^* applied traction coefficient
 ξ Poisson's ratio
 ρ inverse curvature sum, m⁻¹ (in.⁻¹)
 σ_0 maximum surface contact pressure, Pa (psi)
 τ_0 maximum reversing orthogonal shear stress, Pa (psi)
- Subscripts:
- A, B elastic bodies
 i system element
 s system
 x, y reference planes

Analysis

Fatigue Life Model

In 1947 Lundberg and Palmgren (ref. 4) published a statistical theory for the failure distribution of ball and roller bearings. The mode of failure was assumed to be subsurface-originated (SSO) fatigue pitting. Lundberg and Palmgren theorized that SSO fatigue pitting was due to high stresses in the neighborhood of a stress raising incongruity in the bearing material. Their theory is used by bearing manufacturers to establish rolling-element-bearing fatigue-life ratings. In references 5 and 6 the theory was applied to predicting the fatigue lives of spur and helical gears. The predicted life of a steel gearset was confirmed with life data from full-scale spur-gear tests (ref. 6). The theory has also been adapted to analyzing the fatigue lives of traction drives (refs. 2 and 7). The theory that follows is an extension of that presented in reference 3.

For a steel rolling-element the number of stress cycles endured before failure occurs is given by the following equation (ref. 2):

$$L = \left(\frac{K_1 z_0^h}{\tau_0^c V} \right)^{1/e} \quad (1)$$

This modified form of the Lundberg-Palmgren theory for contact-fatigue-life prediction is applicable to gears, bearings, and other rolling-contact elements. The critical shear stress τ_0 is considered to be the maximum orthogonal reversing shear stress, which occurs below the surface of the contacting elements. This stress is not the largest of the subsurface stresses, but it has the largest fluctuating component, which is critical to the fatigue process. The stress volume term V is important since Lundberg-Palmgren theory is based on the probability of encountering a fatigue-initiating flaw in the volume of the material that is being stressed. The depth to the critical stress z_0 is a relative measure of the distance the fatigue crack must travel in order to emerge at the surface and thus cause a failure. For rolling-element bearings (and bodies in rolling contact in general) made of AISI 52100 steel (Rockwell-C 62 hardness), with a fatigue life at a 90-percent probability of survival, the following values are appropriate for use in equation (1) to determine life (in millions of stress cycles):

$$K_1 = 1.430 \times 10^{95} \text{ (N and m units)} \quad = 3.583 \times 10^{56} \text{ (lbf and in. units)}$$

Based on life tests of ball and roller bearings, the accepted exponent values are $h = 7/3$, $c = 31/3$, and $e = 10/9$ for an elliptical point contact or $e = 3/2$ for a line contact (ref. 4).

Contact Stress Analysis

The stress analysis of elastic bodies in contact was developed by Hertz (ref. 8). Hertz assumed homogeneous, solid, elastic bodies made of isotropic material, which are characterized by Young's

modulus E and Poisson's ratio ξ . Bodies A and B in contact are assumed to have quadratic surfaces in the neighborhood of the contact point. The theory of Hertz is summarized by Harris (ref. 9).

Figure 1 shows two bodies in contact. Planes x and y are the respective planes of maximum and minimum relative curvature for the bodies. These planes are mutually perpendicular. They are also perpendicular to the plane that is tangent to the contacting bodies' surfaces at the point of contact. Planes x and y must be chosen so that the relative curvature in plane x is greater than in plane y , thus:

$$\frac{1}{r_{Ax}} + \frac{1}{r_{Bx}} > \frac{1}{r_{Ay}} + \frac{1}{r_{By}} \quad (2)$$

The radii of curvature may be positive or negative depending on whether the surfaces are convex or concave, respectively.

When the bodies are pressed together, the point of contact is assumed to flatten into a small area of contact which is bounded by an ellipse with major axis $2a$ and minor axis $2b$ as shown in figure 1. Plane y contains the major axis of the contact ellipse, and plane x contains the minor axis. The ratio a/b is called the ellipticity ratio of the contact. The values of a/b range from 1 to ∞ for various curvature combinations of contacting surfaces. For cylinders in contact the ellipticity ratio approaches ∞ , and the flattened area of contact is a rectangular strip. For spheres in contact the ellipticity ratio is 1. The first type is called line contact and all other types are called point contacts.

When performing contact analysis, one must be aware of the geometrical orientation of the rolling radii and of principal planes. The principal radii r_{Ax} and r_{Bx} are not, in general, equal to the rolling radii. A typical pair of traction rollers in contact is shown in figure 2. Bodies A and B are generalized traction rollers which rotate, in this case, about coplanar axes. The distance from the axis of rotation of a body to the point of contact is the rolling radius of the body. This is the radius which determines rotational speed and drive ratios. The plane of contact is the plane which is tangent to both bodies at the point of contact. The principal radii r_{Ax} and r_{Bx} lie in the principal plane, which is perpendicular to the plane of contact. Thus, the value of r_{Ax} or r_{Bx} is defined by a line segment that is normal to the contact plane between the point of the contact and some point on the axis of rotation (fig. 2). A trigonometric relationship exists between the principal radii, r_{Ax} and r_{Bx} and the rolling radii, R_A and R_B as a function of the angles between the rotational axes and the contact plane. As shown in the figure, the principal transverse radii r_{Ay} and r_{By} lie in the plane of the cross section which is also perpendicular to the contact plane.

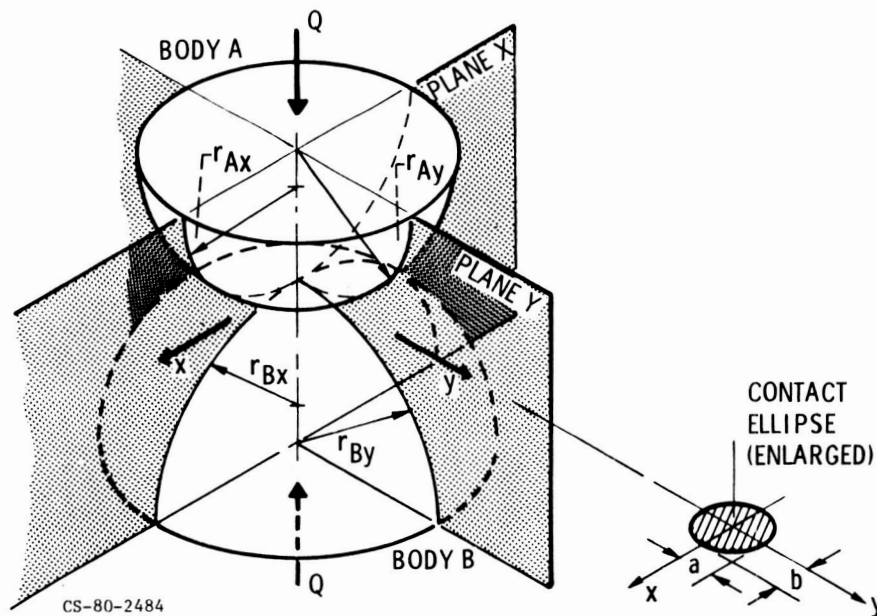


Figure 1. - Geometry of contacting solid elastic bodies.

It is instructive to note that when performing elasto-hydrodynamic (EHD) film thickness calculations or those having to do with traction, the orientation of the contact ellipse relative to the direction of rolling becomes important. While in most applications the semimajor ellipse axis a is oriented perpendicular to the rolling direction, this is not always the case. In many EHD film thickness equations, dimension a is taken to be perpendicular to the rolling direction, irrespective of whether it is the semimajor or semiminor ellipse axis. Since, in this analysis, dimension a is always taken to be the semimajor axis, it may not always correspond to dimension a for purposes of calculating EHD film thickness.

In figure 2 the axes of rotation are in the same plane. This is the case for nearly all traction drives. If the rollers rotate about axes that are significantly skewed in relation to one another or if extreme misalignment exists, then the principal radii must be redetermined on the basis of three mutually perpendicular planes which satisfy equation (2). For slight misalignments the difference in the radii will be very small.

The maximum surface contact pressure at the center of the elliptical pressure distribution is

$$\sigma_0 = \frac{3Q}{2\pi ab} \quad (3)$$

where the semimajor and semiminor contact ellipse axes are

$$a = a^*g \quad (4)$$

$$b = b^*g \quad (5)$$

and the auxiliary contact size parameter is

$$g = \sqrt[3]{\frac{3Q}{2\rho} \left(\frac{1 - \xi_A^2}{E_A} + \frac{1 - \xi_B^2}{E_B} \right)} \quad (6)$$

and where the inverse curvature sum is

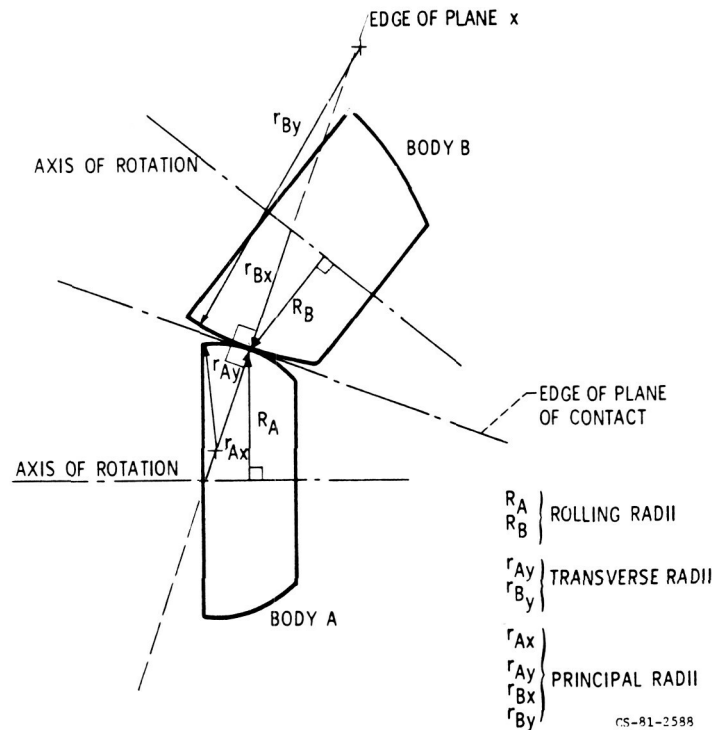


Figure 2. - Geometry of typical traction rollers.

$$\rho = \frac{1}{r_{Ax}} + \frac{1}{r_{Bx}} + \frac{1}{r_{Ay}} + \frac{1}{r_{By}} \quad (7)$$

For steel contacting bodies, with $E_A = E_B = 207$ GPa (3.0×10^7 psi) and $\xi_A = \xi_B = 0.3$, the auxiliary contact size parameter can be expressed as

$$g = 2.36 \times 10^{-4} \sqrt[3]{\frac{Q}{\rho}} \quad (\text{N and m units})$$

or

$$g = 4.50 \times 10^{-3} \sqrt[3]{\frac{Q}{\rho}} \quad (\text{lbf and in. units})$$

The dimensionless contact ellipse semimajor and semiminor axes, a^* and b^* , can be determined from the elliptical integrals used in Hertzian theory (ref. 9). The values of a^* and b^* are plotted in reference 9. Curve-fitted equations for the elliptical integrals can be found in references 7 and 10. The magnitude of the critical stress, that is, the subsurface maximum orthogonal reversing stress τ_0 and its depth z_0 in equation (1), are also given in references 7, 9, and 10. The stressed volume V for a rolling-element contact is given by

$$V = az_0 2\pi |R| \quad (8)$$

where R is the element's rolling radius. This assumes that the semimajor axis a is perpendicular to the rolling direction. Thus, the term $2\pi R$ is equal to the length of the rolling track which is traversed during one revolution.

Fatigue Life Equation

Elliptical contacts. – Estimation of the theoretical fatigue life of a rolling-element contact based on the aforementioned equation is fairly straightforward. By substituting the previously discussed terms into equation (1), a simpler formula can be developed, which expresses the life in terms of material constants, applied load, and contacting body geometry.

Assuming both contacting bodies are made of steel (i.e., $E_A = E_B = 208$ GPa (3.0×10^7 psi) and $\xi_A = \xi_B = 0.3$) and using the exponents and material factor already presented, equations (1) to (8) can be combined to obtain

$$L = K_4 (K_2)^{0.9} Q^{-3} \rho^{-6.3} |R|^{-0.9} \quad (9)$$

where $L = 90$ percent survival life of a single contacting element in millions of stress cycles, and

$$K_2 = \left(\frac{z_0}{b}\right)^{4/3} \left(\frac{\tau_0}{\sigma_0}\right)^{-31/3} (a^*)^{28/3} (b^*)^{35/3} \quad (10)$$

$$K_4 = 2.32 \times 10^{19} \quad (\text{N and m units})$$

$$= 6.43 \times 10^8 \quad (\text{lbf and in. units})$$

where R is the rolling radius of the body whose life is L . The geometry variable K_2 contains four factors, each of which depend only on the relative curvature difference, F , where

$$F = \frac{\left(\frac{1}{r_{Ax}} + \frac{1}{r_{Bx}}\right) - \left(\frac{1}{r_{Ay}} + \frac{1}{r_{By}}\right)}{\rho} \quad (11)$$

From the values of a and b given in reference 9, it can be determined that the contact ellipticity ratio a/b is also a function of F . Thus, given either F or a/b , the variable K_2 can be determined as shown in figure 3.

For convenience an approximation for K_2 can be developed from an expression appearing in Lundberg and Palmgren's (ref. 4) rolling-element bearing capacity equation. After suitable rearrangement of terms, K_2 can be directly calculated from F , by the approximation

$$K_2 = 4.80 \times 10^6 (1 - F)^{-1.367} (1 + F)^{-5.633} \quad (12)$$

As can be seen from the plot of this equation (fig. 4), it is accurate to within 10 percent for $F > 0.8$ or $a/b >$ about 4. For more accurate K_2 values or when $a/b < 4$, figure 4 can be used directly, or equation (10) can be used together with the curve-fitted parameters appearing in references 7 and 10.

In many traction drives the contact ellipse is oriented such that semimajor axis is perpendicular

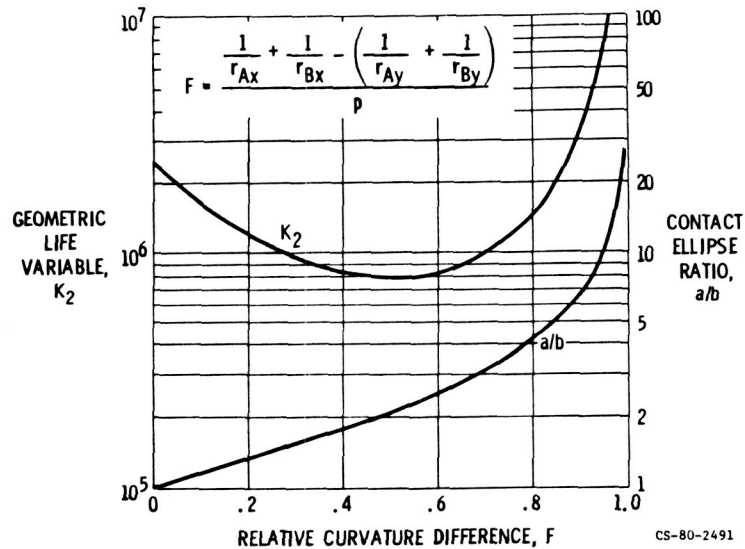


Figure 3. - Geometric life variable K_2 and contact ellipse ratio a/b versus relative curvature difference F .

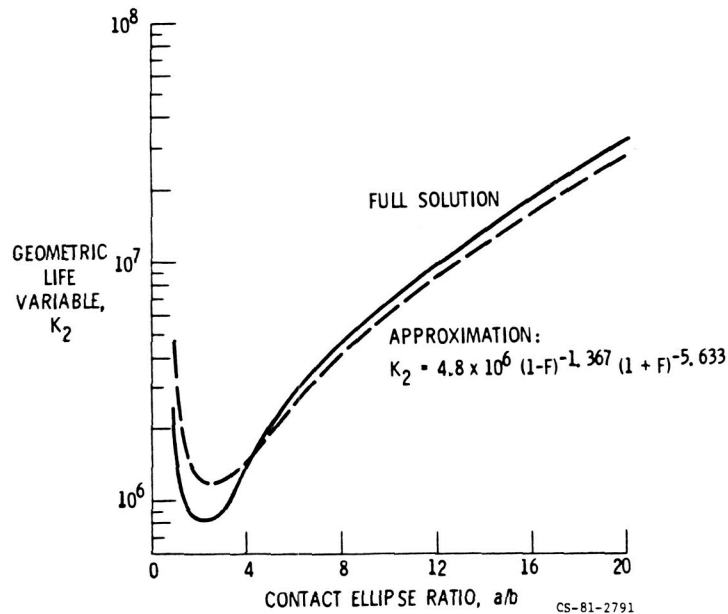


Figure 4. - Approximation for geometric life variable.

to the direction of rolling. If this is the case and if the rolling radii are also equal to the principal radii, that is, $R_A = r_{Ax}$ and $R_B = r_{Bx}$, then

$$\rho = \frac{2}{R_A} \left(\frac{1 + \frac{R_A}{R_B}}{1 + F} \right) \quad (13)$$

and from equation (9)

$$L = K_5(K_2)^{0.9} Q^{-3} \left(\frac{\left| 1 + \frac{R_A}{R_B} \right|}{1 + F} \right)^{-6.3} |R_A|^{5.4} \quad (14)$$

where

$$\begin{aligned} K_5 &= 2.95 \times 10^{17} \text{ (N and m units)} \\ &= 8.16 \times 10^6 \text{ (lbf and in. units)} \end{aligned}$$

and where R_A is the rolling radius of the body whose life in millions of stress cycles is L and R_B is the rolling radius of the mating body.

In the calculation of the stressed volume term V in equation (8), the contact ellipse semimajor axis has been assumed to be oriented perpendicular to the direction of rolling. However, if the semiminor axis is perpendicular to the rolling direction, the stressed volume expression (eq. (8)) must contain the semiminor axis, b , instead of semimajor axis, a . Equations (9) and (10) are still valid with the exception that in equation (10) the exponent of a^* becomes $31/3$ and the exponent on b^* becomes $32/3$. Also figure 4 and the approximation (eq. 12) are no longer valid. Then K_2 can be found from the modified equation (10) together with the curve-fitted parameters of references 7 and 10.

An expression for the maximum surface contact pressure can also be developed for steel bodies from equations (6) to (8) where

$$\sigma_0 = \frac{8.55 \times 10^6}{a^* b^*} Q^{1/3} \rho^{2/3} \text{ (N and m units)}$$

or

$$\sigma_0 = \frac{2.36 \times 10^4}{a^* b^*} Q^{1/3} \rho^{2/3} \text{ (lbf and in. units)} \quad (15)$$

Line contacts. – The analysis presented thus far has been confined to point contact. In the case of the line contact, it can be shown that

$$L = K_6 Q^{-3} |R_A|^{3.22} W^{2.33} \left(\left| 1 + \frac{R_A}{R_B} \right| \right)^{-3.89} \quad (16)$$

where

$$\begin{aligned} K_6 &= 4.21 \times 10^{25} \text{ (N and m units)} \\ &= 6.71 \times 10^{14} \text{ (lbf and in. units)} \end{aligned}$$

and where R_A is the rolling radius of the body whose life, in millions of stress cycles, is L , and R_B is the rolling radius of the mating body.

The expression for maximum surface contact pressure in line contact is

$$\sigma_0 \propto Q^{1/2} \quad (17)$$

and, therefore, from equation (17)

$$L \propto \sigma_0^{-6} \quad (18)$$

However, the sixth power relationship between fatigue life and contact pressure is unlike that of any rolling-contact fatigue data known to the authors. Most data show at least a ninth-power relationship (ref. 11). In reference 6 fatigue tests on spur gears whose contact geometry approximate that of a line contact, life was inversely related to the 8.6 power of stress. Additionally, the Lundberg-Palmgren data, which were used to establish the line-contact exponents, were generated for a roller bearing that assumed a "modified" line contact. This contact was analytically developed from an elliptical contact stress distribution that had been mathematically corrected (ref. 4). Furthermore, it is not desirable to design traction contacts without some transverse curvature. Transverse curvature is required to avoid the adverse effects of excessive edge loading as a result of possible axis skew, misalignment, or overhang. In view of the above the life equation for line contact should be used with discretion.

System life. – Heretofore, the equations express rolling-element fatigue life for a single rolling element in terms of millions of stress cycles. However, in the case of a traction drive, it is system life that is important. All bodies in a system accumulate stress cycles at different rates because their speeds of rotation and number of stress cycles per revolution may not all be the same. To compare lives of the various bodies, clock time should be used. Assume that the speed in revolutions per minute of the i^{th} body is n_i and that there are u_i stress cycles per revolution, then the life of body, i , in hours is given by

$$H_i = \frac{L_i}{u_i n_i} \frac{10^6}{60} \quad (19)$$

The life of the system is then found by applying Weibull's rule (ref. 9). If the system consists of i roll bodies and the life of each is designated H_i ($i = 1$ to j), then the system life in hours is given by

$$H_S = \left[\frac{1}{(H_1)^e} + \frac{1}{(H_2)^e} + \dots + \frac{1}{(H_j)^e} \right]^{-1/e} \quad (20)$$

Thus, for the simplest arrangement, a single pair of rollers, the contact life in hours for an elliptical contact would be

$$H_S = \left[\frac{1}{(H_1)^{10/9}} + \frac{1}{(H_2)^{10/9}} \right]^{-9/10} \quad (21)$$

where H_1 and H_2 are equal to the individual lives of each roller.

Reliability. – The material constant K_1 required in equation (1) was deduced from fatigue-test data at a 90-percent probability of survival. Such a fatigue life is the life which 90 percent of a large number of identical traction drive systems will equal or exceed under a given operative condition. Rolling-element bearing capacities, given in manufacturer's catalogs, are generally defined at this 90-percent life. However, the service life of many gearboxes and other mechanical components is based on some mean or average time before failure. The effect of different reliability levels on rolling-element and traction contact fatigue life is shown in figure 5. Note that at the median life level (50-percent survival) the life is over five times the life at 90-percent survival. Because of the statistical distribution of rolling-element fatigue life, the median fatigue life is not equal to the mean or average life. For the accepted values of the exponent e in equation (1) of 10/9 and 3/2 for ball and roller

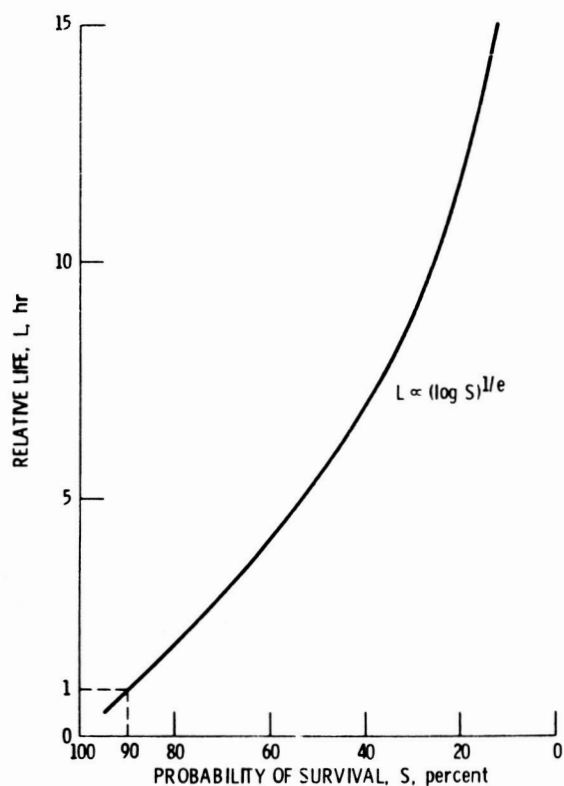


Figure 5. - Relative probability of survival.

bearings, the mean life corresponds to 61.7-percent and 57.6-percent failed, respectively (ref. 12). One should thus be aware of the difference between designing for 90-percent reliability and designing on the basis of mean life, as is the case for many machine elements.

Life Adjustment Factors

Advancements in rolling-element bearing technology since the publication of the Lundberg-Palmgren theory have generally increased bearing fatigue lives. These improvements resulted from the use of improved materials and manufacturing techniques along with a better understanding of the variables affecting fatigue life. In recognition of these advancements, life adjustment factors have been developed (ref. 1) for adjusting Lundberg-Palmgren fatigue-life ratings for ball and roller bearings. Several of these factors are considered to be equally applicable to traction-drive elements in view of the similarities in contact geometry, operating conditions, failure modes, materials, and lubrication (ref. 2). The factors that are appropriate are material, processing, and lubrication.

An additional factor, not considered for rolling-element bearings in reference 1, but important to traction-drive contacts is the potentially deleterious effect that traction may have on fatigue life. The addition of a tangential force component to the contact can alter the subsurface stress field which may, in turn, change the fatigue life. Some investigators (ref. 13) have found a decrease in life from rolling-element fatigue tests when relative sliding and traction are introduced. Rolling-element fatigue tests (ref. 14) with increased spin (i.e., rotational sliding within the contact area) also showed a reduction in fatigue life. However, insufficient data currently exist to properly quantify the effects of traction on rolling-element fatigue life. It is prudent to include in life calculations the possibility of a reduction in fatigue life due to traction. A life factor arbitrarily set to 1/2 would not be unreasonable until better test data are available. In this paper the effects of the operating variables on fatigue life have not been adjusted by the life modifying factors cited. Such factors are much more important on an absolute basis than on a relative basis as used here.

Results and Discussion

Effects of Size, Speed, and Traction Coefficient

The relative effects of roller size and speed on drive system life and torque capacity are of immense interest to the designer of traction drive systems. Generally, for a given power level and life, the size of a power transmitting element, such as a gear or a traction drive roller, can be reduced as speed is increased, since torque decreases. This effect and several others can easily be studied for general and specific cases through the use of equation (9).

Size effects. – It is evident from equation (9) that for a given rolling contact, increasing the load will decrease life by a power of 3. In other words, for a constant available traction coefficient and body size,

$$L \propto T^{-3} \quad (22)$$

In addition, a direct relationship exists between life and element size (radius and contact width). For constant torque and traction coefficient, $Q \propto 1/R$. For constant relative radii difference F , the transverse radius or contact width is proportional to the rolling radius. Therefore, $\text{size} \propto R$. Also, $K_2 = \text{constant}$ and $\rho \propto 1/R$. Substituting these proportionalities into equation (9) and noting that size and rolling radius can be interchanged yield

$$L \propto \left(\frac{1}{\text{size}}\right)^{-3} \left(\frac{1}{\text{size}}\right)^{-6.3} (\text{size})^{-0.9} \quad (23)$$

or

$$L \propto (\text{size})^{8.4}$$

for constant torque and traction coefficient. Similarly, since load Q is directly related to torque and inversely related to radius, we may write: $Q \propto (\text{torque}/\text{size})$. Substituting this into equation (9) and holding life constant produces

$$\text{Torque} \propto (\text{size})^{2.8} \quad (24)$$

The above two relationships are shown graphically in figure 6. It should be emphasized that, while they are very useful for preliminary sizing, they hold only for a constant available traction coefficient. In detailed drive design, the effect of changes in operating conditions on the traction performance of the lubricant must also be considered.

Size, speed, and traction coefficient effects. – Traction data (refs. 15 and 16) for various lubricants show that the maximum available traction coefficient μ decreases with an increase in surface speed and with a decrease in contact pressure. Typical traction data from a twin-disk machine (described in ref. 16) are given in figure 7 where the maximum available traction coefficient μ is plotted versus surface speed for various maximum contact pressures and a contact ellipse ratio of 5. To provide a safe margin against gross slippage, 75 percent of this maximum coefficient is often used as the operating coefficient in a traction drive.

An arbitrary roller pair of constant ratio and $a/b=5$, operating at a given power level, was analyzed for fatigue life. The contacting rollers were assumed to operate, first, under a fixed applied traction coefficient μ^* and, second, with the highest possible traction coefficient based on the data of figure 7. The appropriate value of μ for this comparison was found from an iterative process, since μ is dependent on the contact pressure and speed and vice versa.

Figure 8 shows the effect of size on contact fatigue life. Figure 9 includes the effect of both size and speed. In figure 8 an increase in size increases life as would be expected. Increasing the operating speed in figure 9 accumulates more stress cycles per hour, but since the speed and torque are inversely related for constant power, the decrease in torque and thus normal load is more significant. This results in longer life at higher speeds. Additionally, figure 9 shows that for a constant-life condition, the rolling-traction element size can be reduced with increased rotational speed.

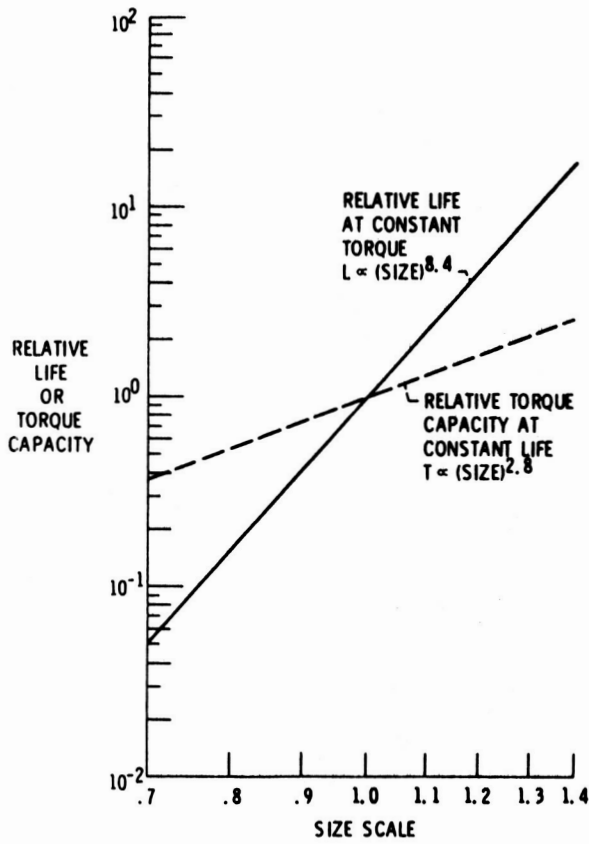


Figure 6. - Relative life at constant torque and relative torque capacity at constant life versus relative size

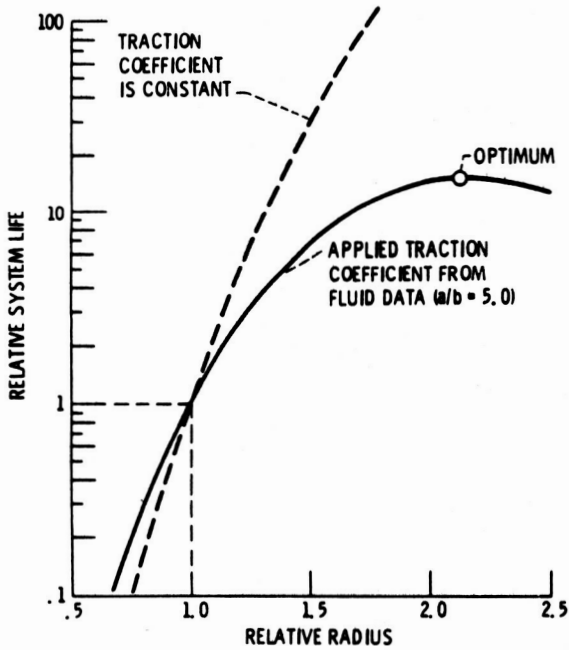


Figure 8. - Relative life versus relative radius for a roller pair in simple traction contact. Power, speed, and a/b are constant.

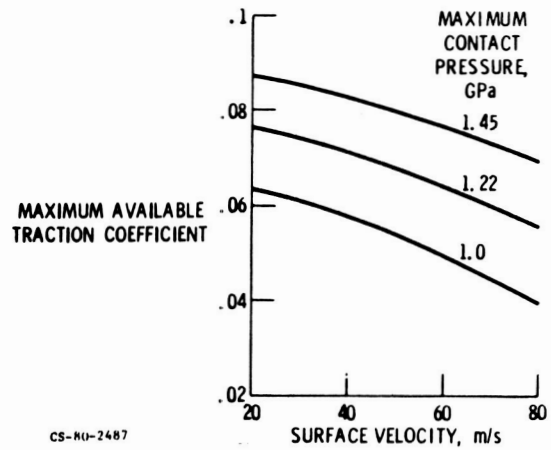


Figure 7. - Typical maximum available traction coefficient versus surface velocity and maximum contact pressure. Synthetic hydrocarbon traction fluid; $a/b = 5$; zero spin; temperature, 343 K. Data from a twin-disk machine described in reference 16.

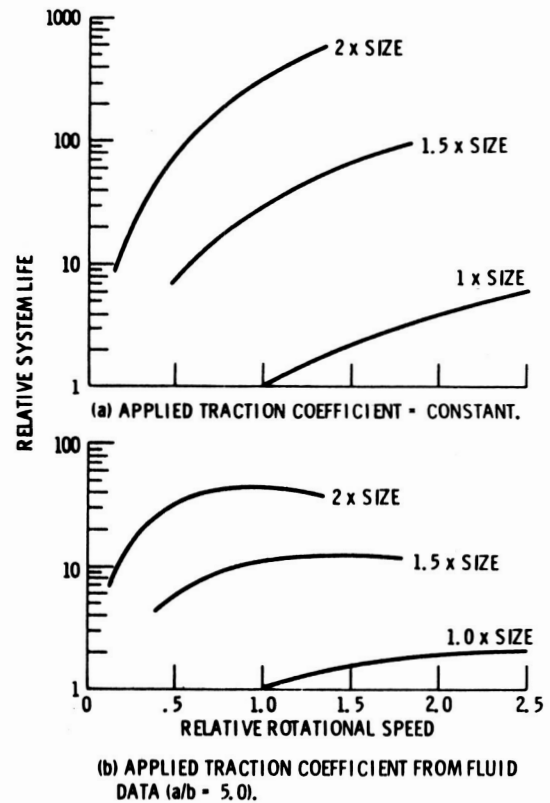


Figure 9. - Relative life versus relative speed for various size roller pairs in simple traction contact. Power, ratio, and a/b are constant.

The reason for higher life in either the constant μ or variable μ case is that increasing a traction roller's size or rotational speed for constant power reduces the tangential force and thus the normal load and contact pressure. However, reducing the contact pressure or increasing the surface speed produces a loss of available traction coefficient and thus a need for a higher normal load to transmit the torque. This loss in μ causes a flattening of the life trend with increased size as shown in figure 8. In fact, for the range shown, the life curve reaches a maximum and then diminishes, indicating an optimum size for best life. Similarly, the life trends in figure 9(b) also flatten due to a loss in μ . The curves of the $1.5\times$ and $2\times$ size rollers show an optimum speed.

The importance of the available traction coefficient to the performance of a traction drive can be related to various design parameters. The drive's overall size (i.e., element diameters), system life, torque capacity, weight, and power-to-weight ratio are quite sensitive to the lubricant's traction coefficient. By substituting $Q = T/\mu$ (where T is the tractive force) into equation (9), the direct effect of traction coefficient on the above parameters can be determined in figure 10, where a/b is held constant. The curves are arbitrarily normalized relative to $\mu = 0.05$. The trend and proportionality between μ and each of the three parameters is valid where the other two parameters are held constant. Life shows the highest sensitivity to μ , but all three performance factors exhibit improvements with higher values of the traction coefficient.

By multiplying the diameter squared by the width of the Hertzian contact, a measure of the drive volume and thus weight can be obtained. The influence of the traction coefficient on relative weight is shown in figure 11. Also shown in figure 11 is the relative power-to-weight ratio, determined by dividing torque capacity at constant speed by weight. These relationships again demonstrate the benefits of using high-traction-coefficient lubricants.

Effect of multiple contacts on capacity and life. – Weight and size efficient traction drives (refs. 17 to 21) generally require multiple, load-sharing contacts. The extent that multiple, parallel contacts reduce unit loading, improve life, and increase power capacity can easily be explored with the analysis presented here. The configurations used to demonstrate this are a set of multiple, identical planetary rollers in external contact with a central sun roller and a set of multiple, identical planetary rollers in internal contact with a ring roller. These arrangements typify the multiple contacts that can

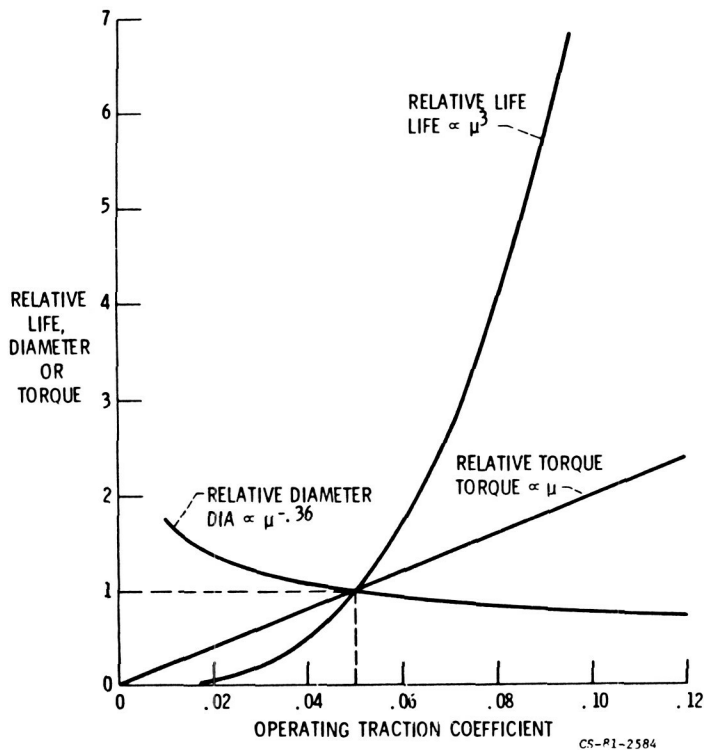


Figure 10. - Relative life, diameter, and torque capacity versus applied traction coefficient.

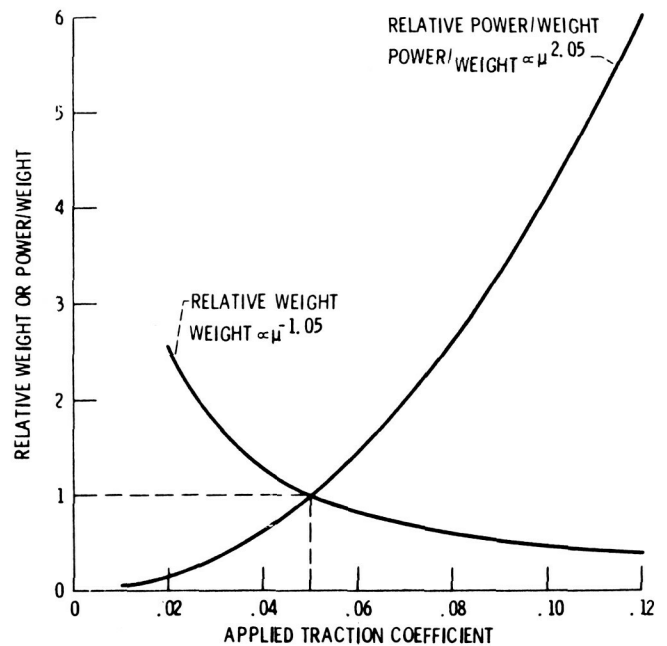


Figure 11. -Relative weight and power-to-weight ratio versus applied traction coefficient.

be found in many types of traction drives.

By beginning with a simple two-roller contact, carrying a certain torque, a multiple roller cluster is formed by adding additional rollers without changing speed, roller size, and sun or ring torque. The life increase and contact pressure decrease for multiple roller contacts are shown in figure 12. Because of the parallel paths, each element is loaded in proportion to the inverse of the number of planets in the cluster. However, life is not proportional to the cube of the number of planets, as equation (9) alone would indicate, because the system life decreases with an increase in the number of components according to equation (18) and because the sun or ring roller experiences more stress cycles per revolution with more planets. Figure 12 is valid for both external and internal contact configurations of any size, ratio, and allowable number of rollers for constant torque, traction coefficient, ellipticity ratio, and element size. An expression for the life as a function of the number of planets can be derived from equation (9) and is given in figure 12. A sample calculation for a three-planet external contact configuration using equation (9) is shown in table 1.

Another advantage of the multiple-contact geometry is the relative compactness of such a traction-drive assembly. Figure 13 shows the relative cluster diameter and contact pressure versus the number of multiple-planet rollers for both external and internal configurations of any ratio operating under constant sun or ring torque conditions at equal system fatigue life. The relative cluster diameter is defined as the ring roller bore diameter or as the pitch diameter of the planet rollers in the case of the sun arrangement. The effect of planet number on the relative sun or ring torque capacity of a certain cluster package size is illustrated in figure 14 for constant size, ratio, traction coefficient, and fatigue life in both external and internal contact arrangements. Figures 12 to 14 show that, for a given application, the maximum number of multiple, load-sharing rollers possible within geometrical ratio limits is advantageous to fatigue life, drive size, and torque capacity.

Application to Multiroller Drive

One high-performance traction drive that has benefitted from multiple, load-sharing elements is the Nasvytis multiroller traction drive (refs. 19 and 21). The drive configuration (fig. 15) consists of

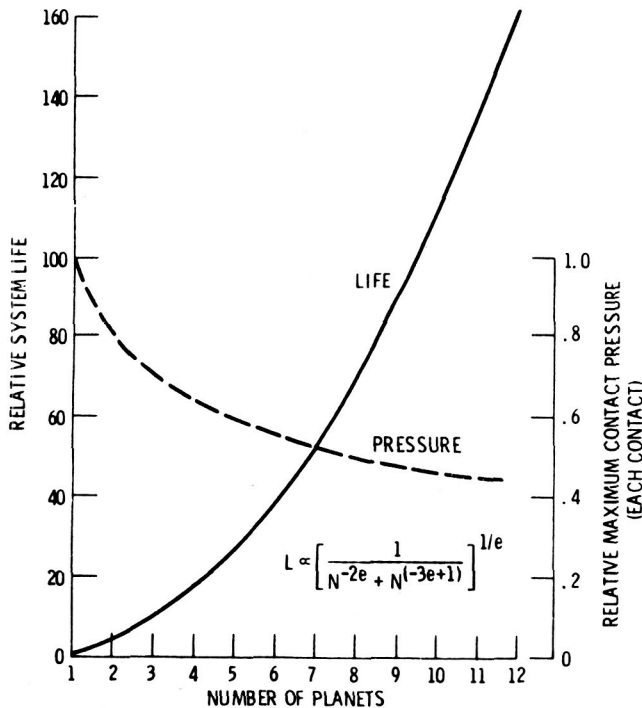


Figure 12. - Relative life and maximum contact pressure versus number of planets for external or internal contact. Torque, element radii, a/b , and traction coefficient are constant.

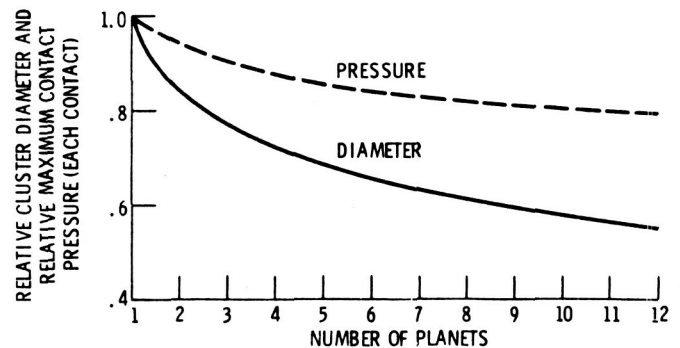
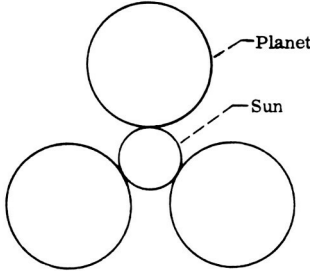


Figure 13. - Relative cluster and relative maximum contact pressure versus number of planets for external or internal contact. System life, a/b , and torque are constant.

TABLE I. - SAMPLE CALCULATIONS

Parameter	Symbol	Formula	Result
<p>Arrangement: External, three load sharing rollers Sun diameter, mm: 25 Planet diameter, mm: 40 Load, each contact, N: 1000 Sun speed, rpm: 10 000 Transverse radii, sun, mm: 500 Transverse radii, planets, mm: 100</p> 			
Normal load, each contact, N	Q	-----	1000
Orthogonal principal radii, m	r_{Ax}	Must satisfy: $\left. \begin{aligned} & \frac{1}{r_{Ax}} + \frac{1}{r_{Bx}} > \frac{1}{r_{Ay}} + \frac{1}{r_{By}} \end{aligned} \right\}$	0.0125
	r_{Ay}		0.5
	r_{Bx}		0.025
	r_{By}		0.1
	Inverse curvature sum, m^{-1}		ρ
Relative curvature difference	F	$\frac{\frac{1}{r_{Ax}} + \frac{1}{r_{Bx}} - \left(\frac{1}{r_{Ay}} + \frac{1}{r_{By}} \right)}{\rho}$	0.818
Geometric life variable	K_2	Fig. 4	1.65×10^6
Sun rolling radius, m	R_{sun}	-----	0.0125
Sun life, millions of cycles	L_{sun}	$K_4(K_2)^{0.9} Q^{-3} \rho^{-6.3} R_{sun}^{-0.9}$	2.07×10^4
Sun stress, cycles/rev	u_{sun}	-----	3
Sun speed, rpm	n_{sun}	-----	10 000
Sun life, hr	H_{sun}	$\left(\frac{L}{un} \right)_{sun} \left(\frac{10^6}{60} \right)$	11 500
Planet rolling radius, m	R_{pl}	-----	0.025
Planet life, millions of cycles	L_{pl}	$K_4(K_2)^{0.9} Q^{-3} \rho^{-6.3} R_{pl}^{-0.9}$	1.11×10^4
Planet stress, cycles/rev	u_{pl}	-----	1
Planet speed, rpm	n_{pl}	-----	5000
Planet life, hr	H_{pl}	$\left(\frac{L}{un} \right)_{pl} \left(\frac{10^6}{60} \right)$	37 000
System life, hr (without adjustment factors)	H_s	$\left[\left(\frac{1}{H_{sun}} \right)^{10/9} + 3 \left(\frac{1}{H_{pl}} \right)^{10/9} \right]^{-9/10}$	6700

concentric sun and ring elements with two rows of planet rollers. The planets do not orbit, but are located on bearings which take reaction torque to the case. Either the sun or ring can act as the input, depending on whether a speed reducer or increaser is desired. A complete life analysis was performed in reference 7, a portion of which is repeated here. The specific drive analyzed was approximately 21 cm in overall diameter and 6 cm wide with a nominal 14.7-to-1 ratio. Table 2 from reference 7 summarizes the calculation results and life-adjustment factors for three typical points, which cover a range of operating conditions up to the maximum rated condition of 194 kW (200 hp) at 75 000 rpm input speed. It is apparent from table 2 that these factors vary relatively little over the entire operating condition spectrum. Also listed is the Lundberg-Palmgren life at each contact, the contact life adjusted for life factors, and the adjusted drive system life. Figure 16 from reference 7 shows the

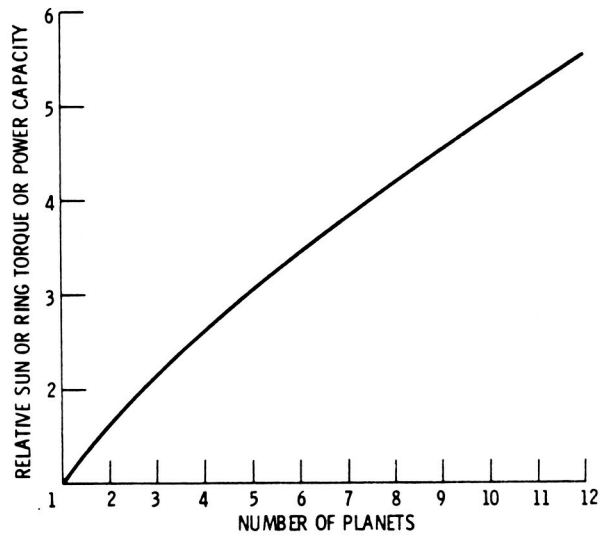


Figure 14. - Relative torque or power capacity versus number of planets for external or internal contact. System life, a/b, and rolling radii are constant.

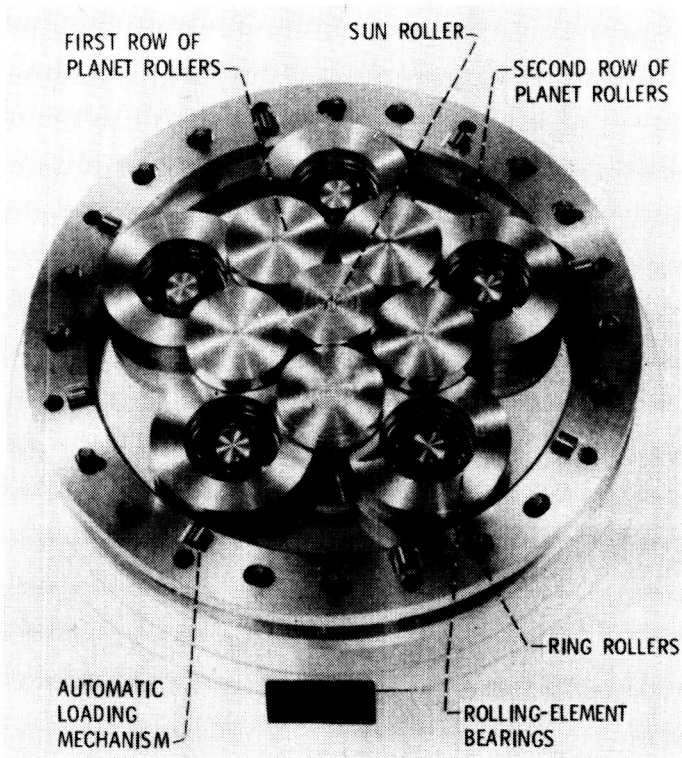


Figure 15. - Basic geometry of a Nasvytis multiroller traction drive.

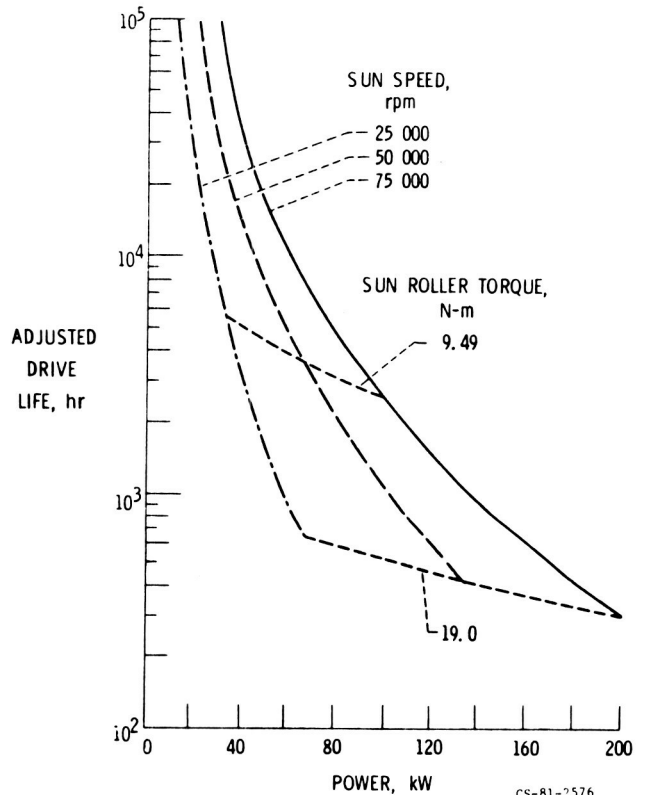


Figure 16. - Adjusted drive system life versus power and speed.

life over a range of input speeds and power levels based on the contact fatigue life theory and life adjustment factors.

TABLE II. - SUMMARY OF CONTACT CONDITIONS, LIFE ADJUSTMENT FACTORS AND DRIVE LIFE FOR THREE DRIVE OPERATING CONDITIONS

	Sun-first planet	First-second planet	Second planet-ring	Sun-first planet	First-second planet	Second planet-ring	Sun-first planet	First-second planet	Second planet-ring
	16.6 kW (22.2 hp) 25 000-rpm sun speed			74.6 kW (100 hp) 75 000-rpm sun speed			149 kW (200 hp) 75 000-rpm sun speed		
Material and processing factor	6	6	6	6	6	6	6	6	6
Surface speed, m/sec	36.6	14.3	14.5	110	43.0	43.5	110	43.0	43.5
Normal load, N	978	1361	2296	1470	2040	3440	2940	4080	6890
Maximum contact pressure, GPa	1.11	1.18	0.950	1.27	1.35	1.09	1.60	1.70	1.37
Film thickness, μm	1.14	0.489	0.972	1.14	1.07	1.14	1.14	1.02	1.14
h/σ	4.0	1.70	3.39	4.0	3.72	4.0	4.0	3.54	4.0
Lubrication factor	2.65	1.85	2.55	2.65	2.6	2.65	2.65	2.6	2.65
Traction factor	0.5	0.5	0.5	0.5	0.5	0.5	0.5	0.5	0.5
Total life adjustment factor	7.95	5.55	7.65	7.95	7.80	7.95	7.95	7.80	7.95
Lundberg-Palmgren life, hr	11 400	4040	1.41×10^6	1130	399	139 000	141	49.9	17 400
Adjusted life, hr	90 600	22 400	1.08×10^7	3980	3110	1.11×10^6	1120	389	138 000
Adjusted drive life, hr	18 800			2440			305		

Summary

A simplified calculation method for predicting the rolling-element fatigue life of traction drive systems with elliptical contacts was presented. It is a useful design tool for properly establishing traction drive size and torque capacity based on fatigue life. A modified form of the Lundberg-Palmgren theory is used as the basis of this fatigue-life model. This life model considers stress, stressed volume, and depth to the critical shear stress as well as the effect of multiple contacting elements. The method was applied to a simple pair of rolling-element traction bodies transmitting a constant power level over a range of element sizes and rotational speeds. The effects of available traction coefficient as a function of contact pressure and surface speed were also investigated. The relationship between available traction coefficient and the design parameters of life, diameter, torque capacity, weight, and power-to-weight ratio were determined.

The method was also applied to systems of multiple, load-sharing rollers in external (sun) and internal (ring) contact arrangements. The system fatigue life for the Nasvytis multiroller traction drive, including life adjustment factors, was reviewed. The following results were obtained.

1. Traction drive size, life, and torque capacity per unit size improve with an increase in number of multiple load-sharing rollers.

2. For a given power and size, the fatigue life of a traction contact increases with an increase in speed. Similarly, for a given power and speed, the fatigue life increases with an increase in size. However, an optimum size or speed exists, beyond which the loss in traction coefficient causes a loss in life.

3. High-traction-coefficient lubricants are beneficial to traction drive life, diameter, torque capacity, weight, and power-to-weight ratio.

References

1. Bamberger, E. N.; et al.: Life Adjustment Factors for Ball and Roller Bearings: An Engineering Design Guide, American Society of Mechanical Engineers, 1971.
2. Coy, John J.; Loewenthal, Stuart H.; and Zaretsky, Erwin V.: Fatigue Life Analysis for Traction Drives with Application to a Toroidal Type Geometry. NASA TN D-8362, 1976.
3. Rohn, D. A.; Loewenthal, S. H.; and Coy, J. J.: Simplified Fatigue Life Analysis for Traction Drive Contacts. J. Mech. Des., vol. 103, no. 2, Apr. 1981, pp. 430-439.

4. Lundberg, G.; and Palmgren, A.: Dynamic Capacity of Rolling Bearings. *Ingenioersvetenskapsakademien, Handlingar*, no. 196, 1947.
5. Coy, J. J.; Townsend, D. P.; and Zaretsky, E. V.: Dynamic Capacity and Surface Fatigue Life for Spur and Helical Gears. *J. Lubr. Technol.*, vol. 98, no. 2, Apr. 1976, pp. 267-274; discussion, pp. 275-276.
6. Townsend, D. P.; Coy, J. J.; and Zaretsky, E. V.: Experimental and Analytical Load-Life Relation for AISI 9310 Steel Spur Gears. *J. Mech. Des.*, vol. 100, no. 1, Jan. 1978, pp. 54-60.
7. Coy, John J.; Rohn, Douglas A.; and Loewenthal, Stuart H.: Life Analysis of Multiroller Planetary Traction Drive. NASA TP-1710, 1981. (AVRADCOR TR-80-C-16.)
8. Hertz, H.: The Contact of Elastic Solids. Part V—Miscellaneous Papers. The MacMillan Company (London), 1896, pp. 146-162.
9. Harris, Tedric A.: *Rolling Bearing Analysis*. Wiley, 1966.
10. Brewe, David E.; and Hamrock, Bernard J.: *Simplified Solution for Point Contact Deformation Between Two Elastic Solids*. NASA TM X-3407, 1976.
11. Parker, R. J.; Zaretsky, E. V.; and Bamberger, E. N.: Evaluation of Load-Life Relation with Ball Bearings at 500 Deg F. *J. Lubr. Technol.*, vol. 96, no. 3, July 1974, pp. 391-397; discussion, pp. 397-409.
12. Johnson, Leonard G.: *The Statistical Treatment of Fatigue Experiments*. Elsevier Publishing Co., 1964.
13. MacPherson, P. B.: The Pitting Performance of Hardened Steels. ASME Paper No. 77-DET39, Sept. 1977.
14. Zaretsky, Erwin V.; Anderson, William J.; and Parker, Richard J.: The Effect of Contact Angle on Rolling-Contact Fatigue and Bearing Load Capacity. *ASLE Trans.*, vol. 5, no. 1, Apr. 1962, pp. 210-219.
15. Hewko, L. O.; Rounds, F. G., Jr.; and Scott, R. L.: Tractive Capacity and Efficiency of Rolling Contacts. *Rolling Contact Phenomena*, Joseph B. Bidwell, ed., Elsevier Publishing Co., 1962, pp. 157-182; discussion, pp. 182-185.
16. Johnson, K. L.; and Tevaarwerk, J. L.: Shear Behaviour of Elastohydrodynamic Oil Films. *Proc. R. Soc., London, ser. A*, vol. 356, no. 1685, Aug. 24, 1977, pp. 215-236.
17. Nasvytis, Algirdas L.: Multiroller Planetary Friction Drives. SAE Paper No. 660763, Oct. 1966.
18. Hewko, Lubomyr O.: Roller Traction Drive Unit for Extremely Quiet Power Transmission. *J. Hydronaut.*, vol. 2, no. 3, July 1968, pp. 160-167.
19. Loewenthal, Stuart H.; Anderson, Neil E.; and Nasvytis, Algirdas L.: Performance of a Nasvytis Multiroller Traction Drive. NASA TP-1378. (AVRADCOR TR-78-36.)
20. Nakamura, Kenya; et al.: A Development of the Traction Roller System for a Gas Turbine Driven APU. SAE Paper No. 790106, Feb. 1979.
21. Loewenthal, S. H.; Anderson, N. E.; and Rohn, D. A.: Evaluation of a High Performance Fixed-Ratio Traction Drive. *J. Mech. Des.*, vol. 103, no. 2, Apr. 1981, pp. 410-417; discussion, pp. 417-422.